united nations
educational, scientific
and cultural
organization

international atomic
energy agency

the
abdus salam
international centre for theoretical physics

SMR 1161/37

AUTUMN COLLEGE ON PLASMA PHYSICS

25 October - 19 November 1999

Laboratory Studies of Magnetic Reconnection, Dynamo Effects, and Magnetic Helicity

Hantao Ji

Princeton University
Princeton Plasma Physics Laboratory
U.S.A.

Laboratory Studies of Magnetic Reconnection, Dynamo Effects, and Magnetic Helicity

By

Hantao Ji

Princeton Plasma Physics Laboratory
Princeton University

Presented at

Trieste Plasma Autumn College
Nov. 8 – 10, 1999

What is Magnetic Reconnection?

Magnetic reconnection is the topological change of a magnetic configuration through re-arrangement of field lines.

An example: plasma merging.

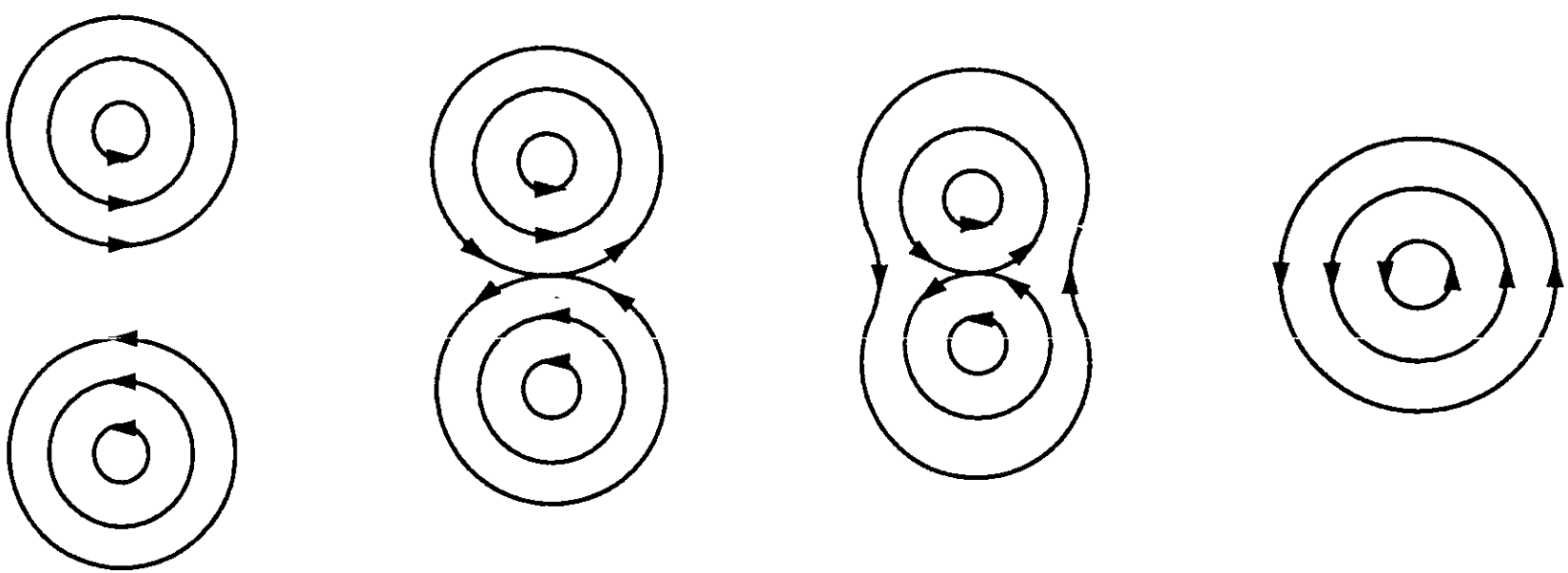

Magnetic Reconnection

- It occurs during the formation and/or configuration changes of solar flares.

  => considered to play a key role in coronal heating, coronal mass ejections, ...

- It occurs when solar wind interacts with the earth magnetic field at the magnetopause and magnetotail.

  => considered to determine magnetic structure around the earth, aurora phenomena...

- It occurs in laboratory plasmas such as sawtooth activities in tokamaks.

  => often determines plasma confinement characteristics, plasma relaxation, dynamo phenomena...

Magnetic Reconnection in Solar Flares

Observations: 15 min. to a few hours

Explanations:

- Pre Sweet-Parker (< '50) time:

  Existence of magnetic field was known but its diffusion time (in 1D) can be as long as a few million years.

- '50 - '60:

  Sweet-Parker Model: simplest classical model of local 2D reconnection. But it predicts a reconnection of a few months.

- '60 - '80:

  Petschek Model: introduces a much smaller diffusion region connected with external fields by a shock structure. It predicts a minimum reconnection time as short as less than an hour.

- '80 - present:

  - Some inconsistency found in Petschek Model
  - Reconnection time can be shortened by using "anomalous" resistivity in Sweet-Parker Models.
  - Debates continue.

  (MRX results)

Sweet-Parker Model

- Local 2D picture
- Steady state ($\partial B/\partial t = 0$):

$$\frac{\partial B}{\partial t} = \nabla \times (V \times B) + \frac{\eta}{\mu_0}\nabla^2 B \quad \Longrightarrow \quad V_R = \frac{\eta}{\mu_0 \delta}$$

- Incompressibility ($\nabla \cdot V = 0$):

$$\frac{\partial \bar{n}}{\partial t} + \bar{n}\nabla \cdot V = 0 \quad \Longrightarrow \quad \frac{L}{\delta} = \frac{V_Z}{V_R}$$

- Pressure balance ($p_{\rm up} = p_{\rm down}$):

$$p_{\rm up} + \frac{B_Z^2}{2\mu_0} + \frac{1}{2}\rho V_R^2 = p_0 = p_{\rm down} + \frac{B_Z^2}{2\mu_0} + \frac{1}{2}\rho V_Z^2 \quad \Longrightarrow \quad V_Z = V_A$$

- Combine them:

$$\frac{V_R}{V_A} = \frac{1}{\sqrt{S}}, \qquad S = \frac{\mu_0 L v_A}{\eta}.$$

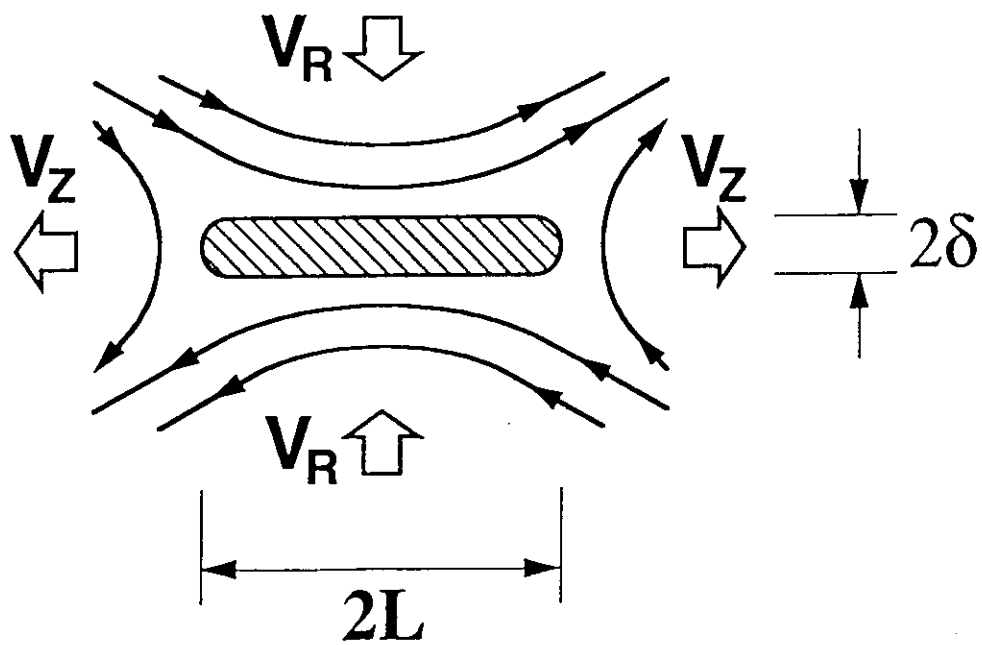

MRX

Assembly
Front View

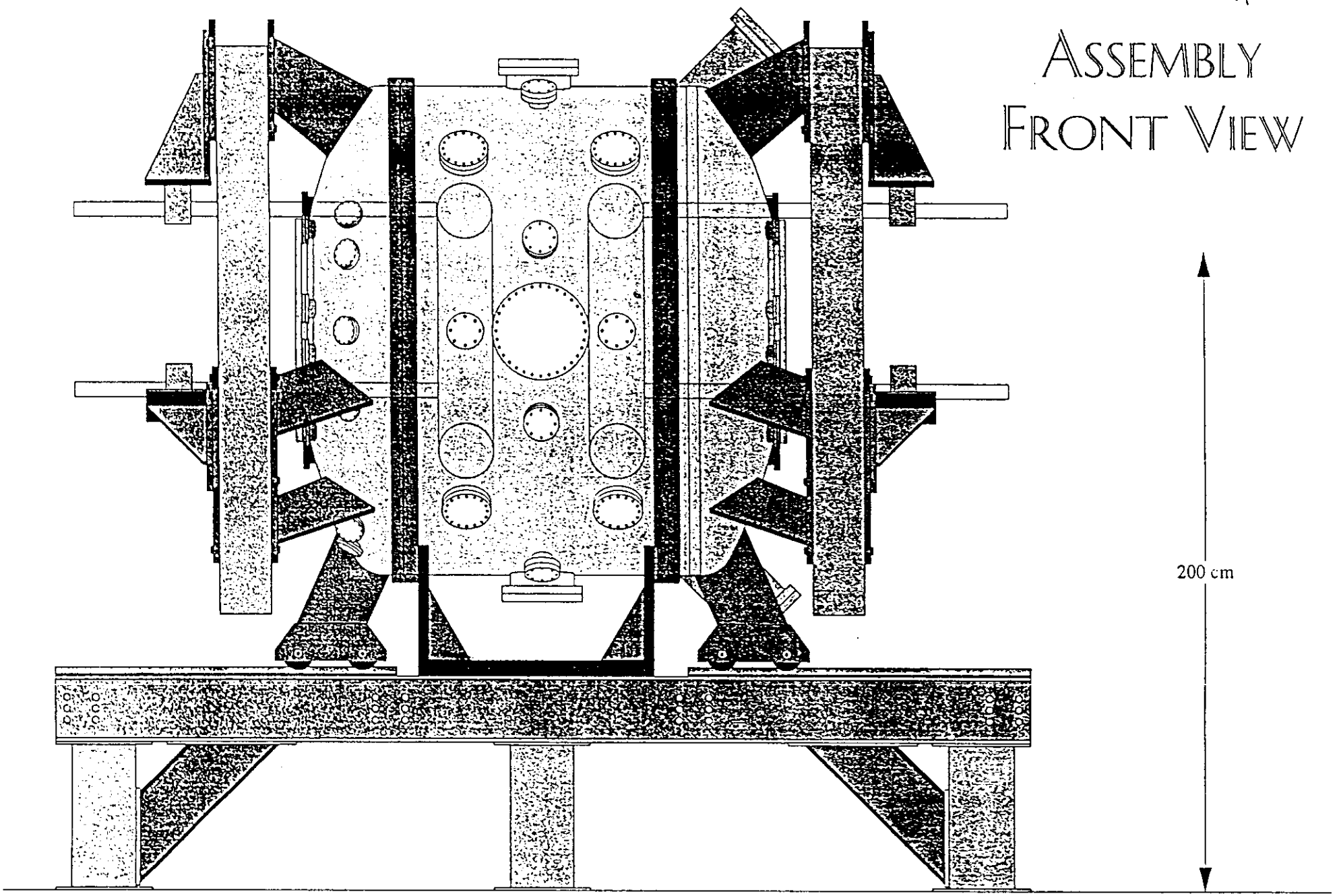

Advantages of MRX as a Reconnection Experiment

- A well-controlled experiment
  - where
  - when
  - but not how: the purpose of experiments
- A well-diagnosed experiment
  - 2D magnetic profiles
  - plasma density (Langmuir probe, interferometer)
  - electron temperature (Langmuir probe, possibly EBW)
  - ion temperature (spectroscopy, LIF)
  - ion flow (Mach probe, spectroscopy, LIF)

Plasma parameters:

$B < 1kG$

$n = (0.1\text{-}2) \times 10^{20}/m^3$, Te=5-25 eV, Ti=10-40eV

S=100-1000

Magnetic Reconnection Experiment

Case 1. Double annular plasma configuration

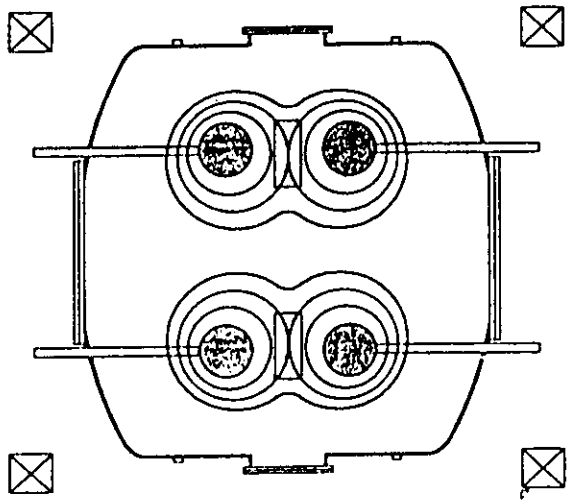

Case 2. Double spheromak configuration

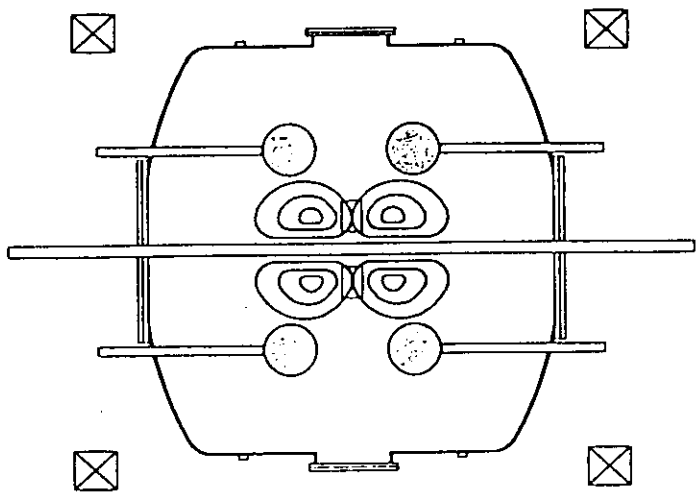

"Push" and "pull" reconnection in the double annular configuration

No reconnection
when $dI_{PF}/dt = 0$

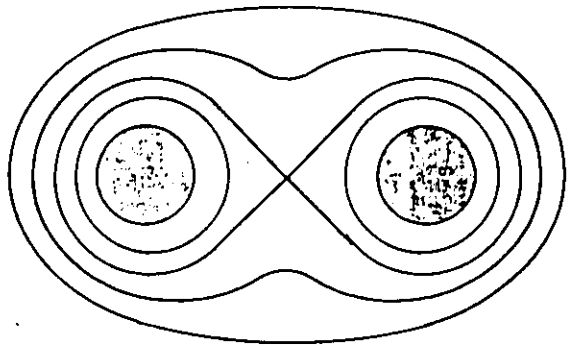

"Push" reconnection
when $dI_{PF}/dt > 0$

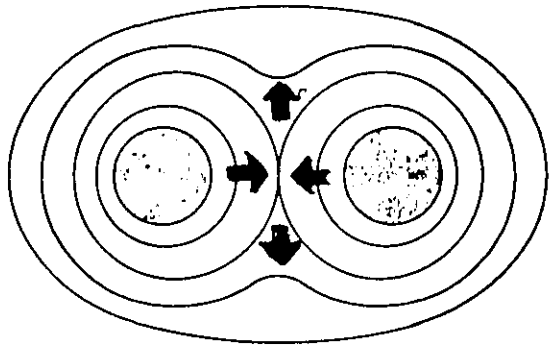

"Pull" reconnection
when $dI_{PF}/dt < 0$

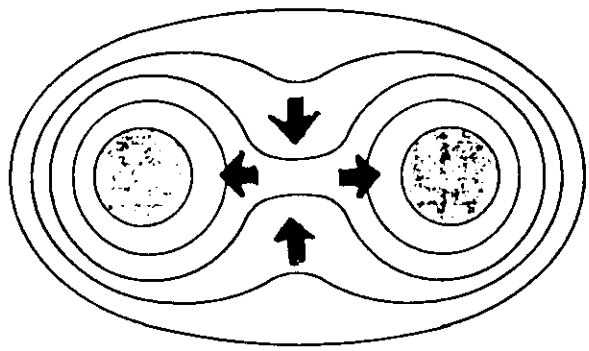

Experimental Setup in MRX

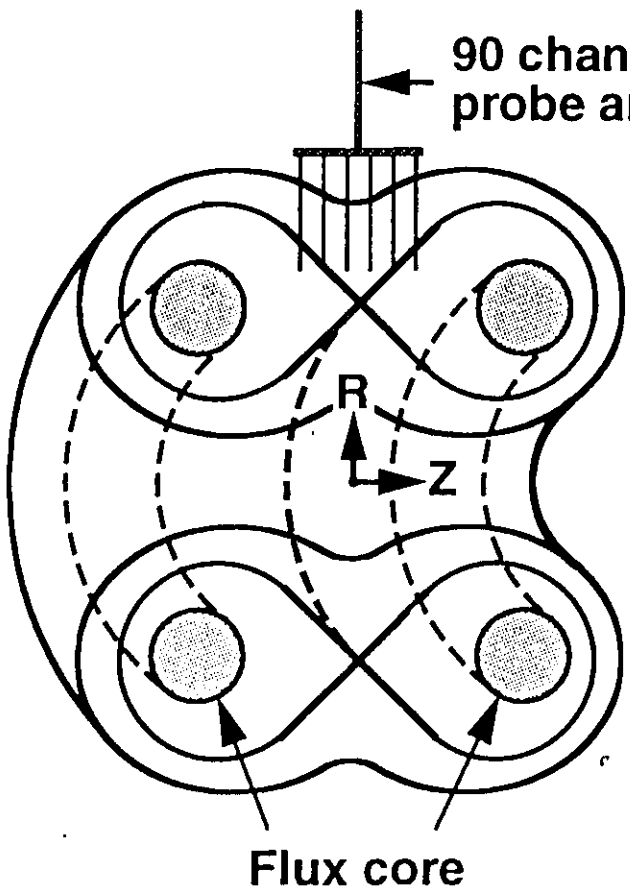

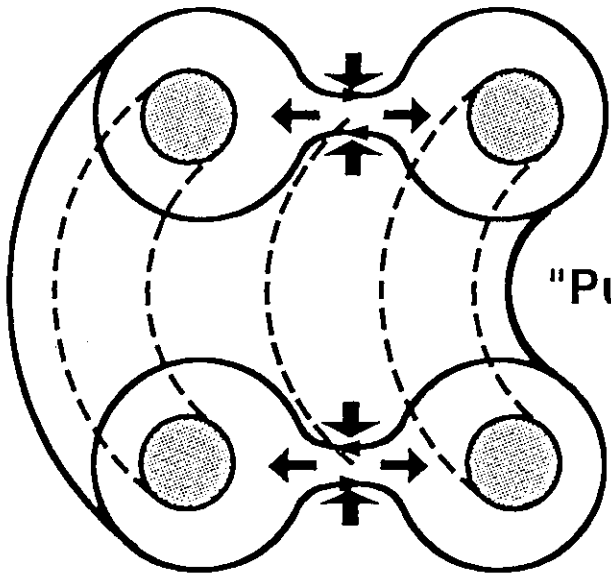

Realization of 2D Magnetic Reconnection in MRX

Measured flux contours (third component B_t=0)

null-helicity

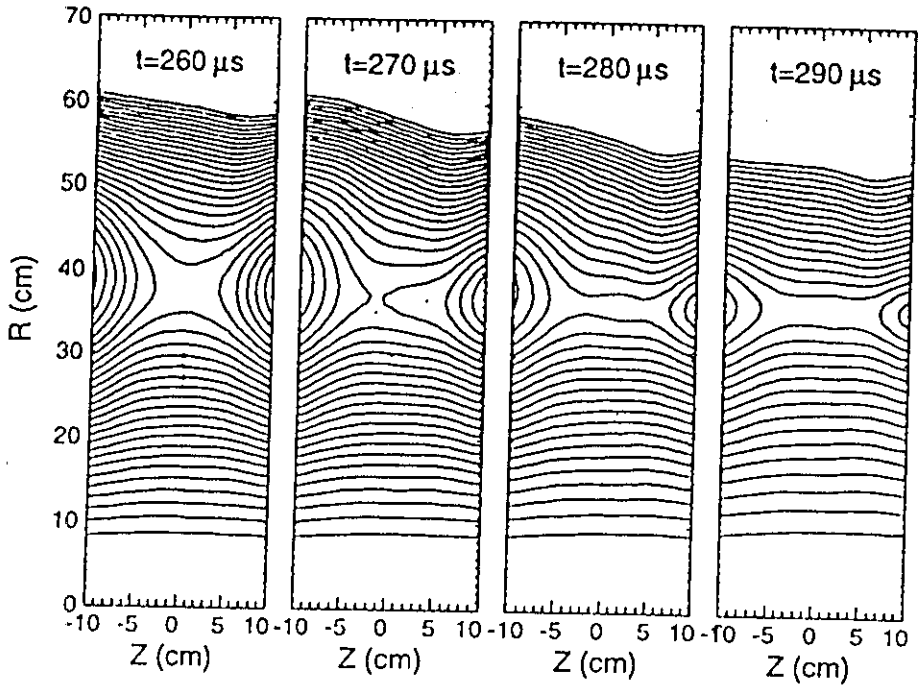

Measured profiles

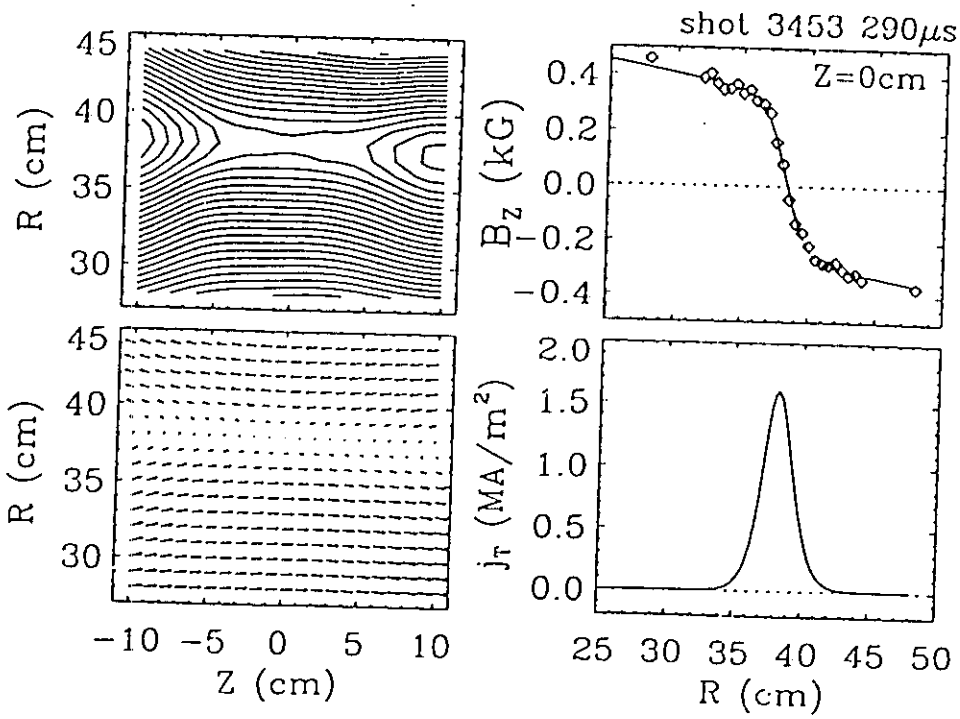

Harris Sheet:

$B \propto \tanh \frac{R-R_0}{\delta}$

$j \propto \mathrm{sech}^2 \frac{R-R_0}{\delta}$

$p \propto \mathrm{sech}^2 \frac{R-R_0}{\delta}$

Time Evolution of Key Physical Quantities

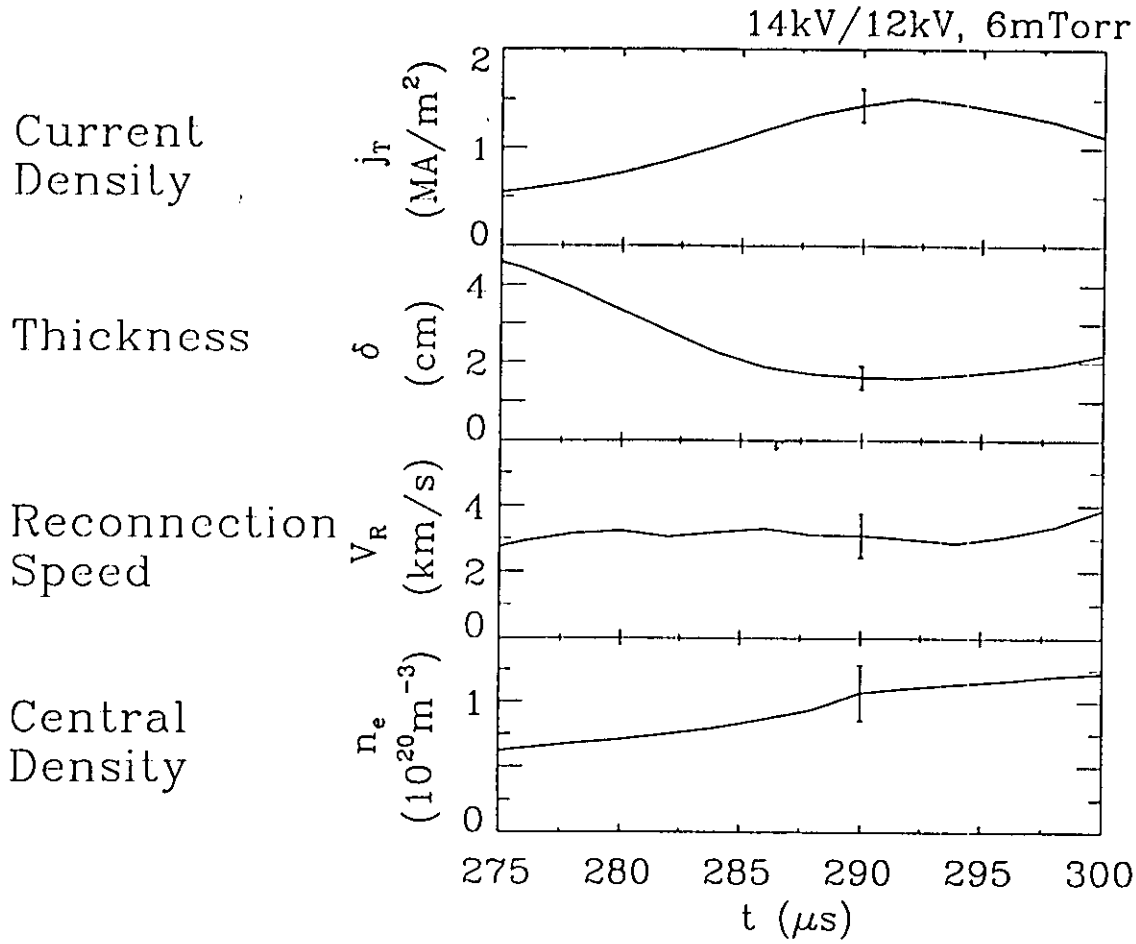

A Straightforward Test of Sweet-Parker Model

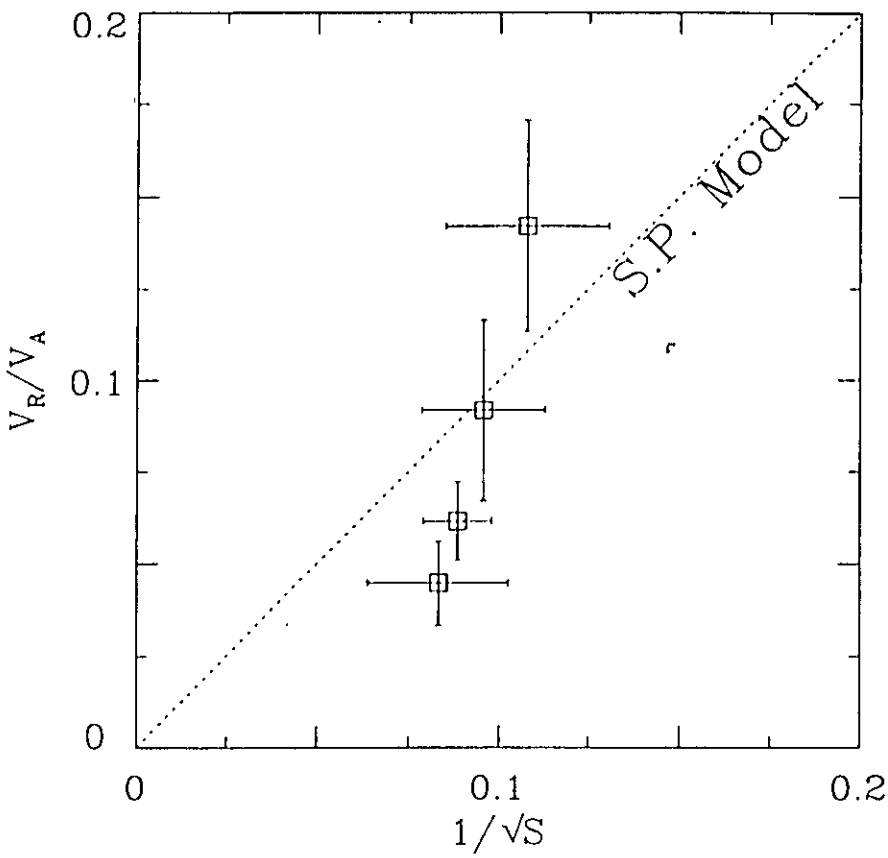

Determination of Resistivity along the Neutral Line

- All three terms are measured in the MHD Ohm's law along the neutral line:

$$E_T + V_R \times B_Z = \eta_\perp j_T$$

- The resistivity is determined by E_T/j_T since $V_R \times B_Z$ is negligible in the center of the diffusion region.

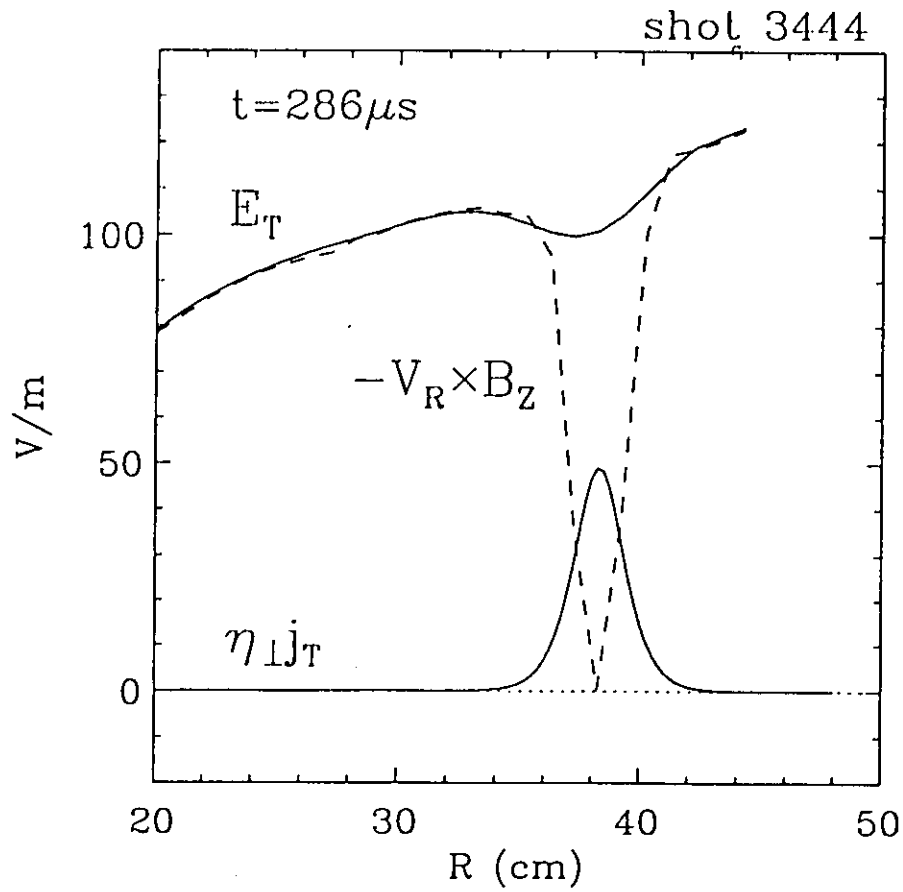

Resistivity Enhancement in Collisionless Regime

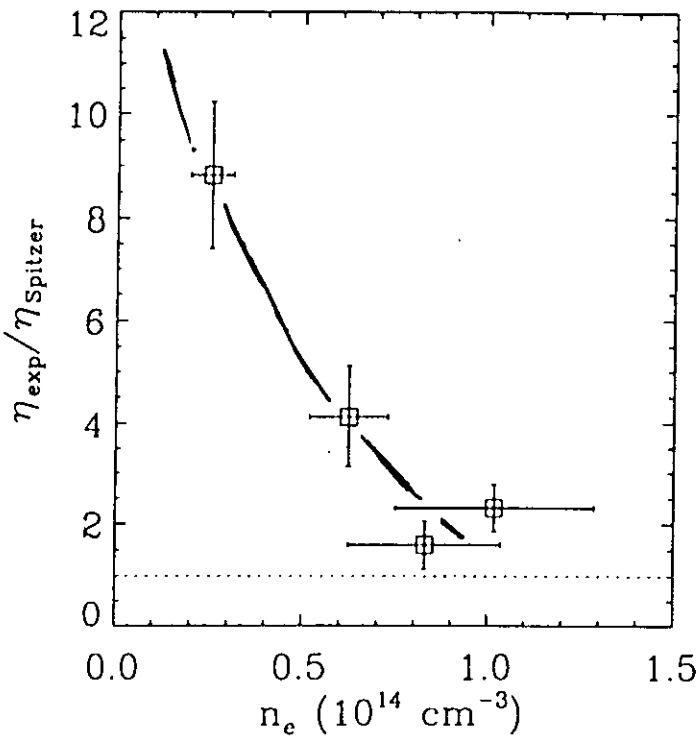

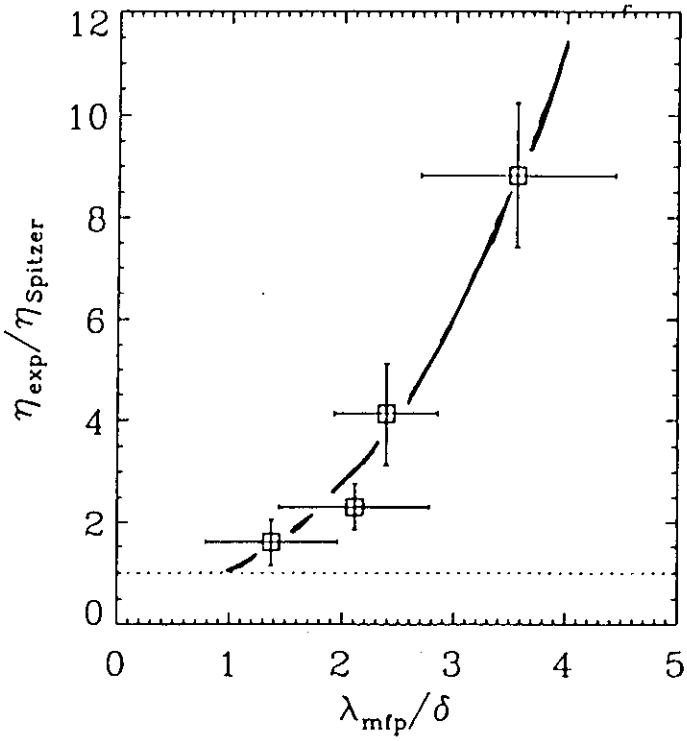

Test of Sweet-Parker Model: Using Effective Resistivity $\eta_\perp^* (= E_T/j_T)$

$$S^* = \mu_0 L V_A / \eta_\perp^*$$

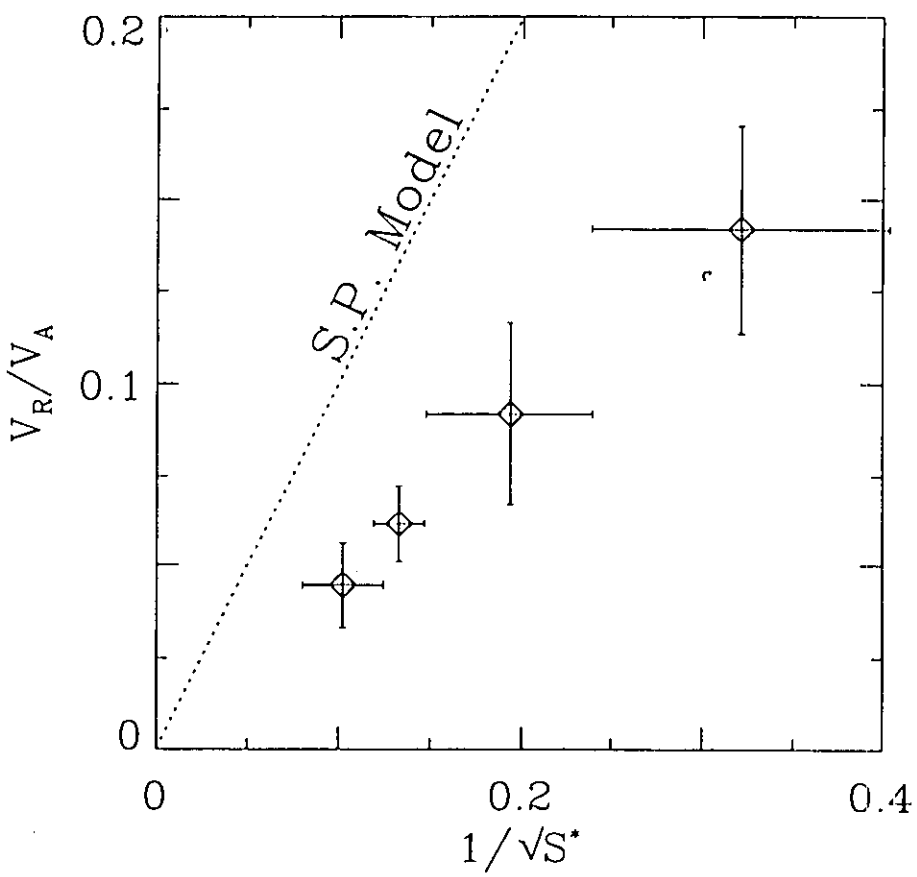

Approximately Steady-state Reconnection

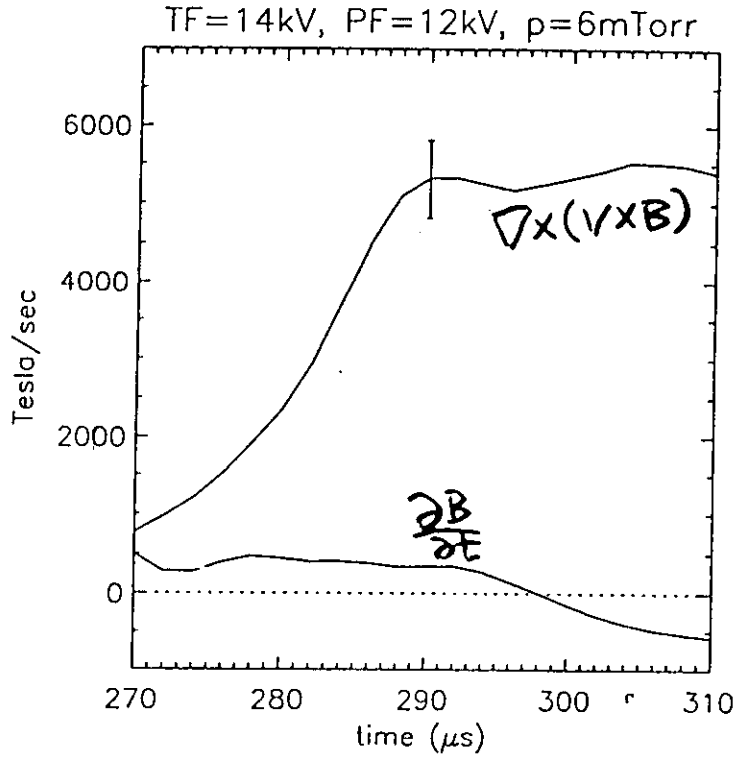

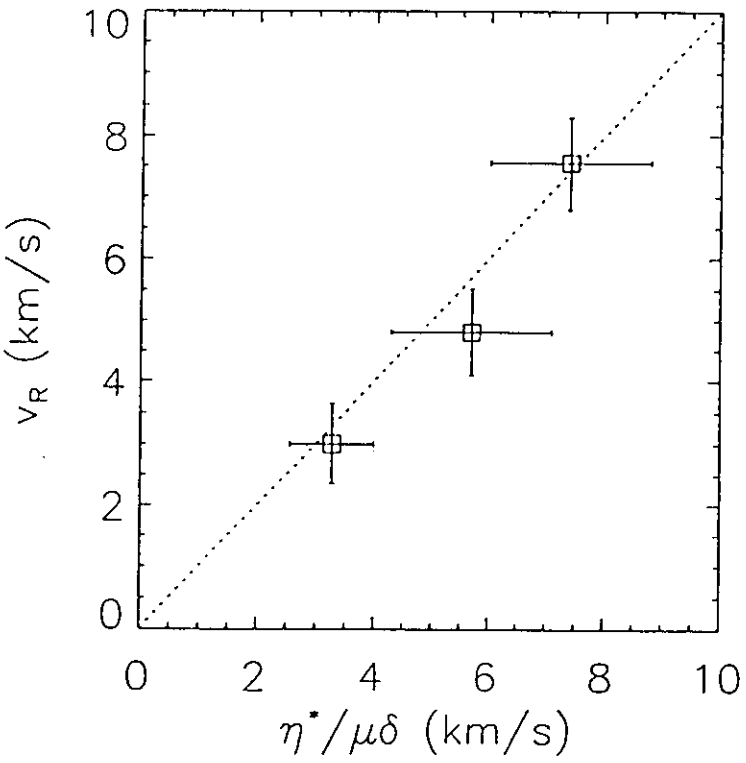

Effect of Compressibility Is Not Negligible

- Compressibility ($\nabla \cdot V \propto \partial n/\partial t > 0$) increases inflow V_R:

$$V_R = \frac{\delta}{L}(V_Z + \underline{\frac{L}{n}\frac{\partial n}{\partial t}}) \quad > \quad \frac{\delta}{L}V_Z$$

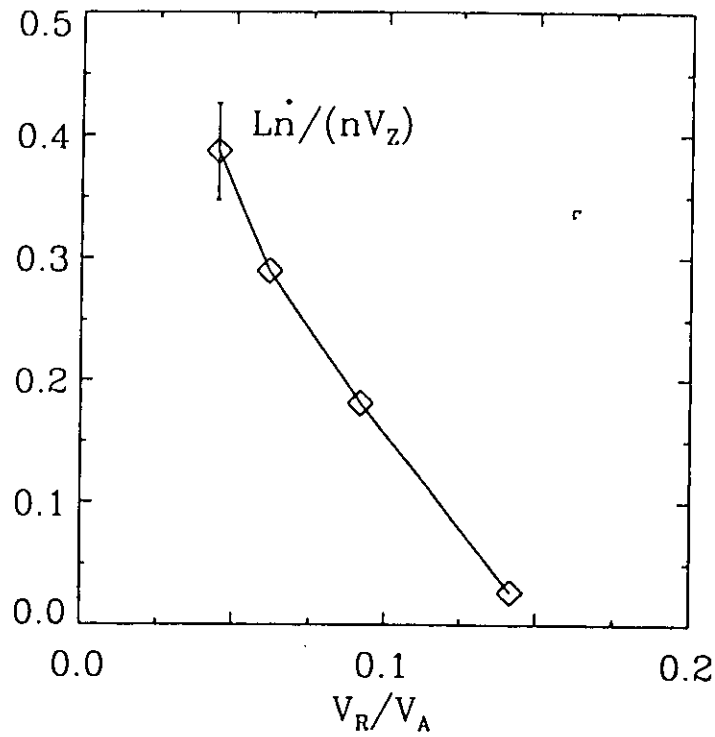

Effect of Down-stream Pressure Is Significant

- Large down-stream pressure ($p_{\rm down} \simeq p_0 \gg p_{\rm up}$) slows outflow V_Z:

$$V_Z = \sqrt{V_A^2(1+\kappa) - 2(p_{\rm down} - p_{\rm up})/\rho} \quad < \quad V_A$$

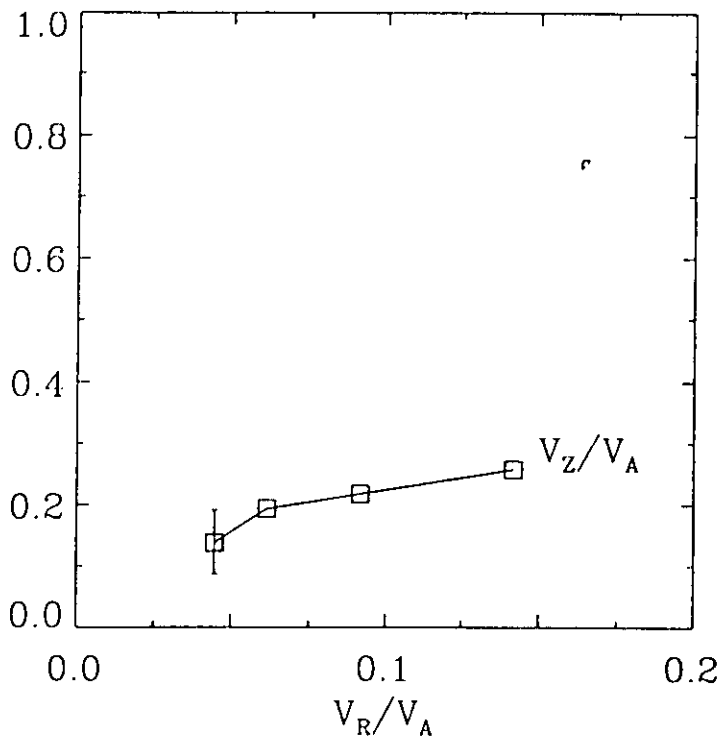

Time Evolution of Density

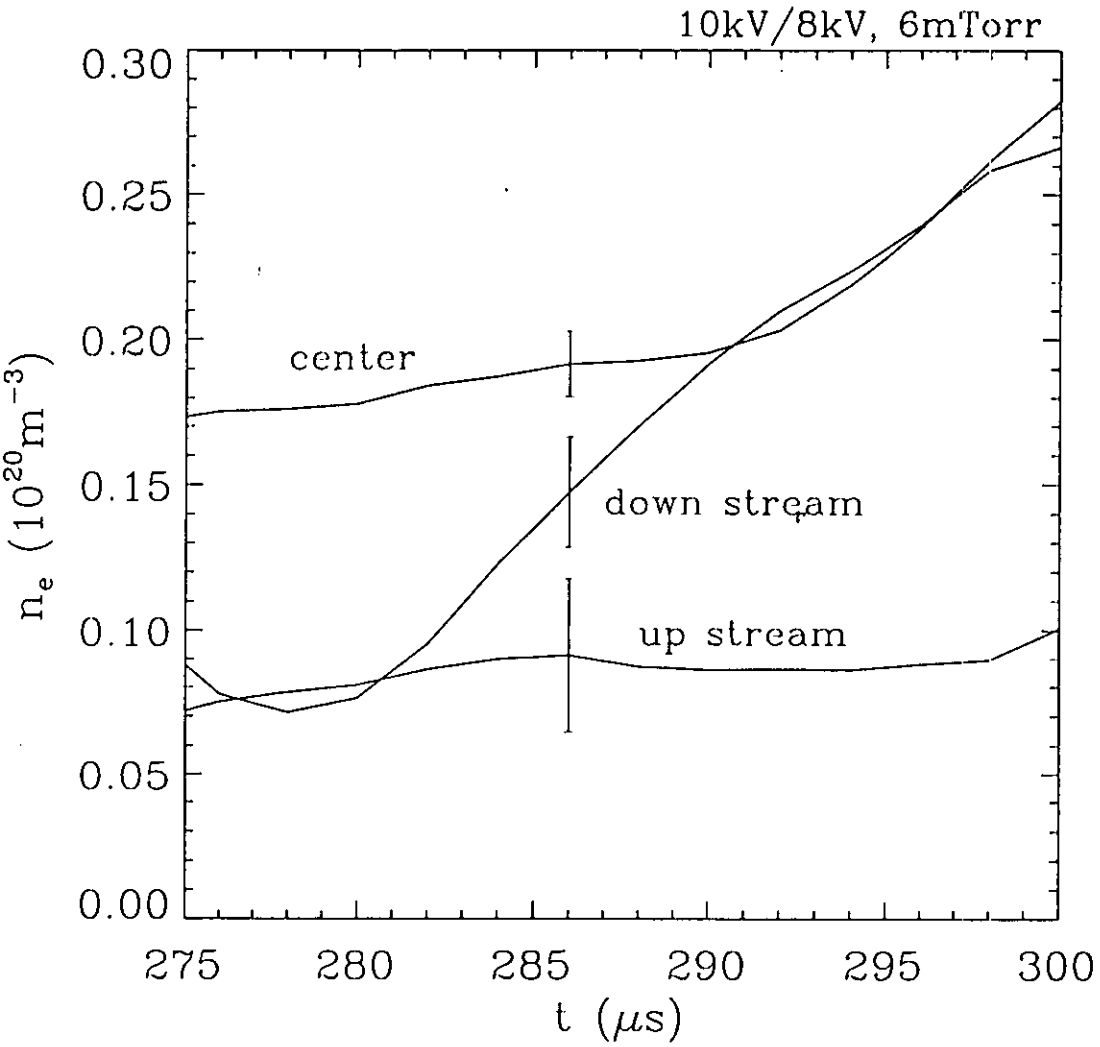

Effect of Down-stream Magnetic Tension Force Is Moderate

- The original Sweet-Parker model neglects the magnetic tension force which is not obviously small:

$$p_{\rm up} + \frac{B_Z^2}{2\mu_0} \;=\; p_0 \;=\; p_{\rm down} + \frac{1}{2}\rho V_Z^2 - \frac{1}{\mu_0}\int_0^L B_R \frac{\partial B_Z}{\partial R} {\rm d}Z$$

$$\Longrightarrow \quad V_Z = \sqrt{V_A^2(1+\kappa) - 2(p_{\rm down} - p_{\rm up})/\rho}$$

where $\kappa \equiv \dfrac{2}{B_Z^2}\displaystyle\int_0^L B_R \frac{\partial B_Z}{\partial R}{\rm d}Z$ represents its relative importance.

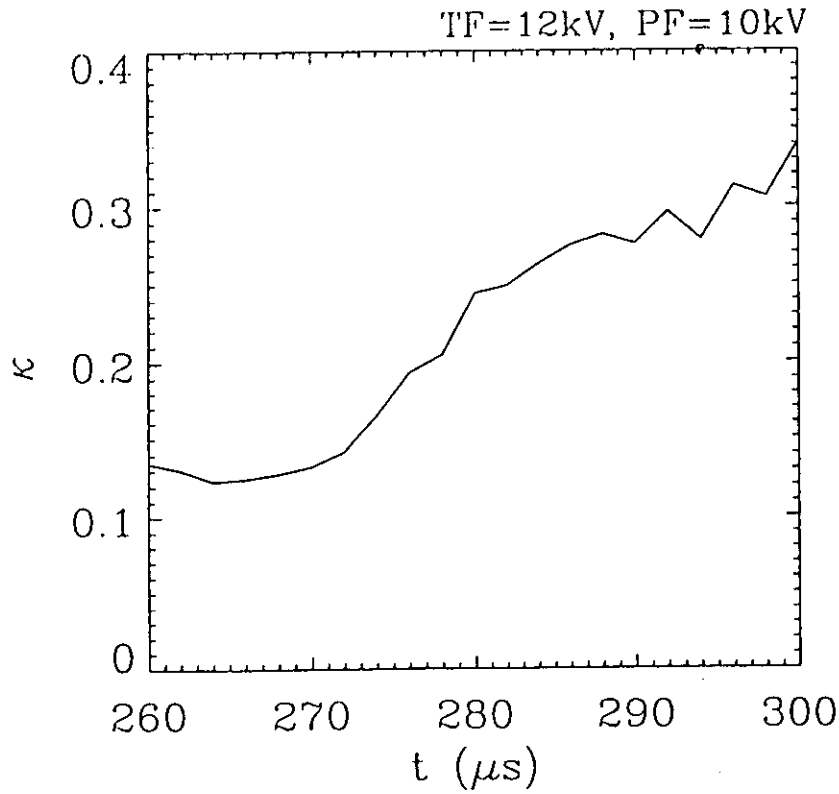

Generalized Sweet-Parker Model

- Steady state ($\partial \boldsymbol{B}/\partial t = 0$):

$$\frac{\partial \boldsymbol{B}}{\partial t} = \nabla \times (\boldsymbol{V} \times \boldsymbol{B}) + \frac{\eta^*}{\mu_0} \nabla^2 \boldsymbol{B} \approx 0 \quad \Longrightarrow \quad V_R = \frac{\eta^*}{\mu_0 \delta}$$

- Compressible ($\boldsymbol{\nabla} \cdot \boldsymbol{V} \propto \partial \bar{n}/\partial t \neq 0$):

$$V_R = \frac{\delta}{L}\left(V_Z + \frac{L}{n}\frac{\partial n}{\partial t}\right)$$

- Non-negligible down-stream pressure ($p_{\rm up} \neq p_{\rm down}$):

$$V_Z = \sqrt{V_A^2(1+\kappa) - 2(p_{\rm down} - p_{\rm up})/\rho}$$

- Combine them:

$$\frac{V_R}{V_A} = \frac{1}{\sqrt{S_{\rm eff}}}, \qquad S_{\rm eff} = \frac{\mu_0 L V_A}{\eta^*} \cdot \frac{1}{1 + L\dot{n}/(nV_Z)} \cdot \frac{V_A}{V_Z}.$$

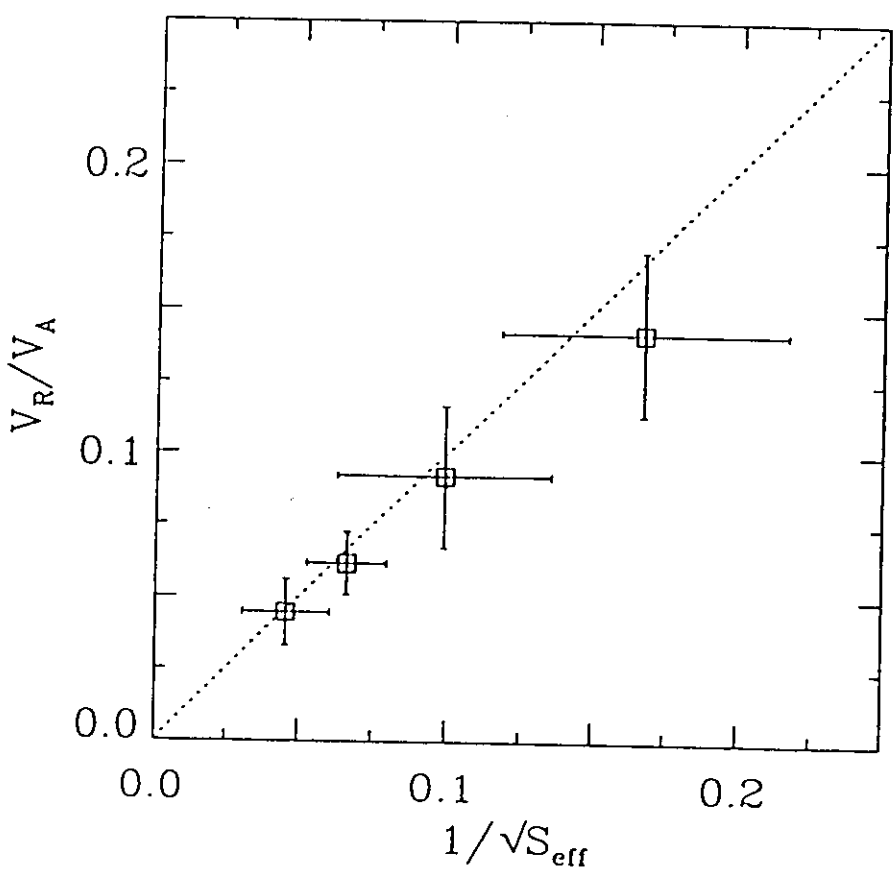

Third Component Decides Reconnecting Angle

Null-helicity (Bt=0)

Co-helicity (Bt~Bp)

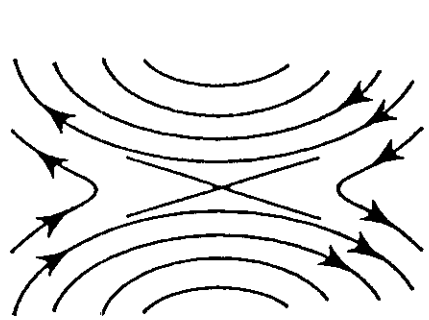

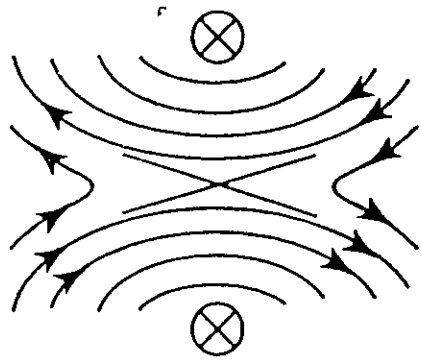

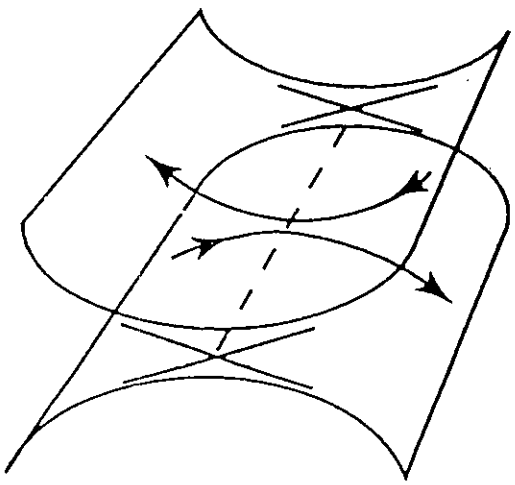

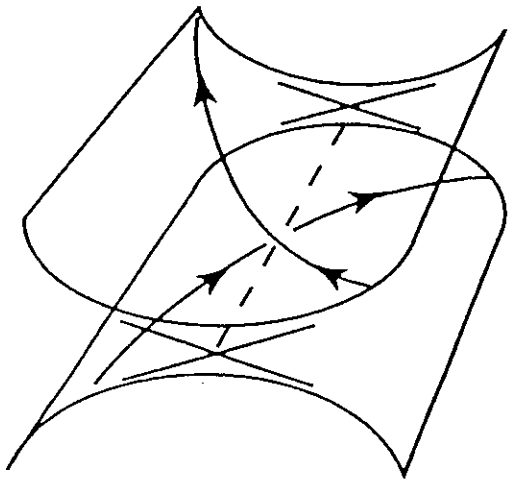

Effects of the Third Component

Null-helicity (Bt = 0) :

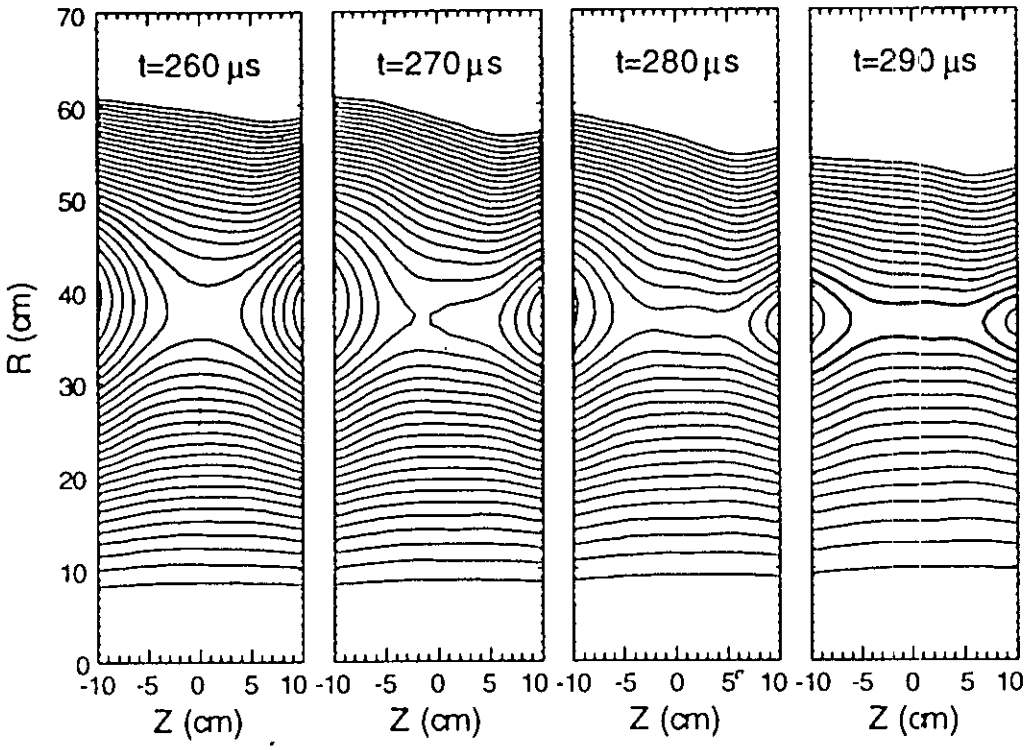

Co-helicity (Bt ~ Bp) :

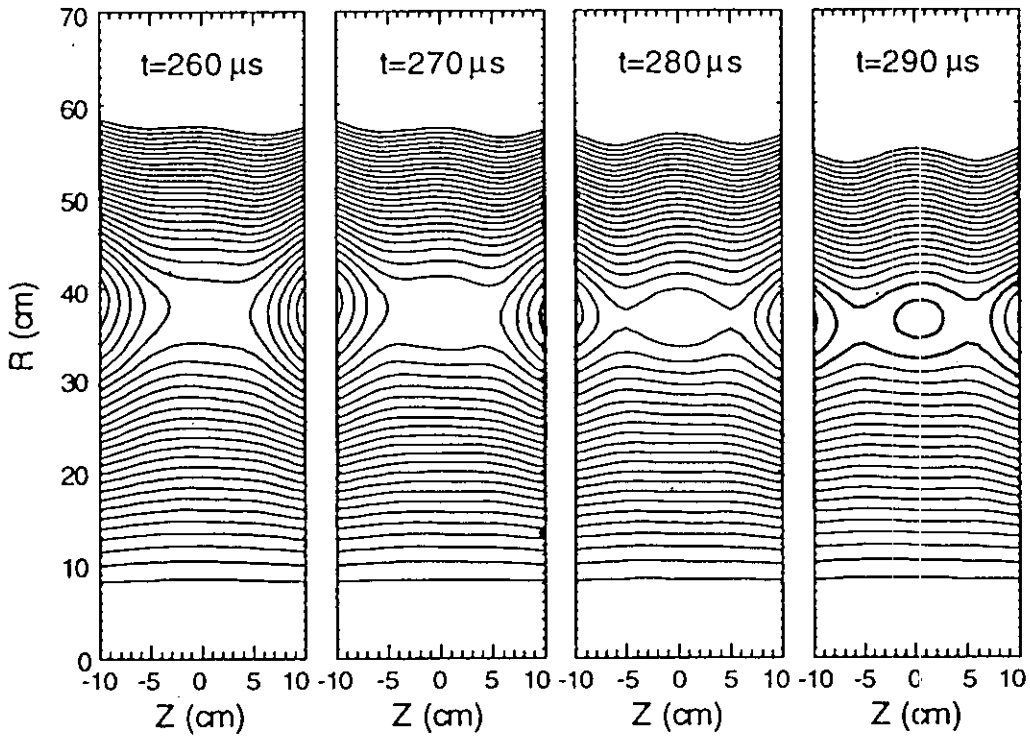

Generalized Sweet-Parker Model Applies to Co-helicity Reconnection

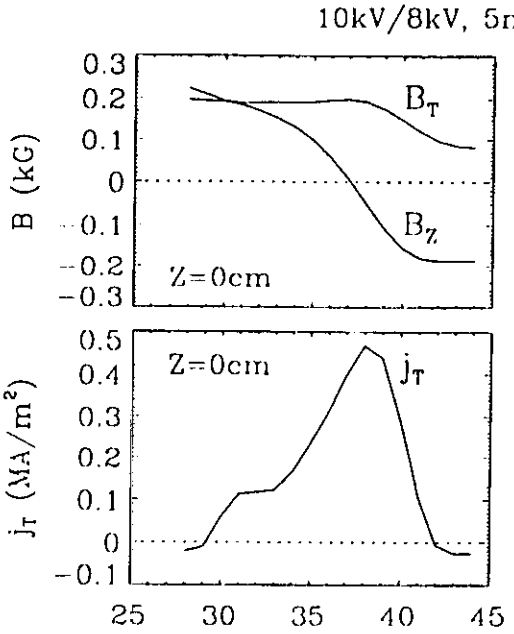

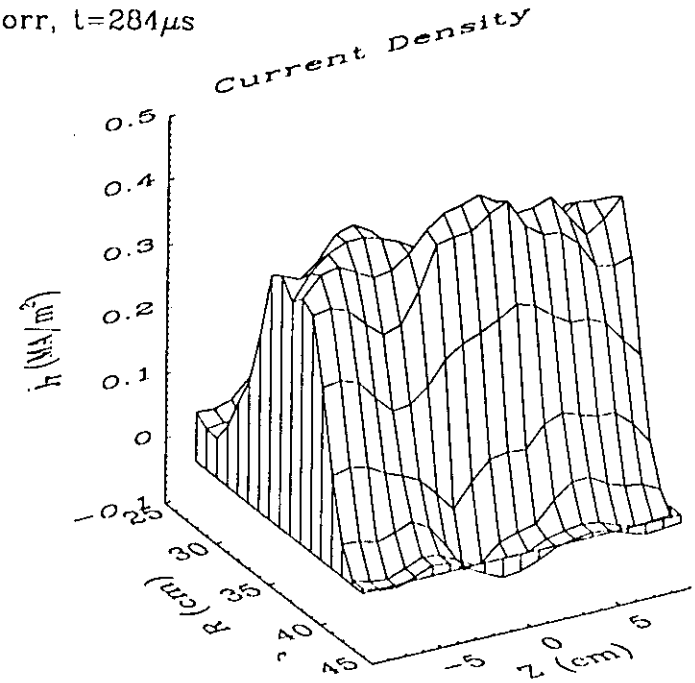

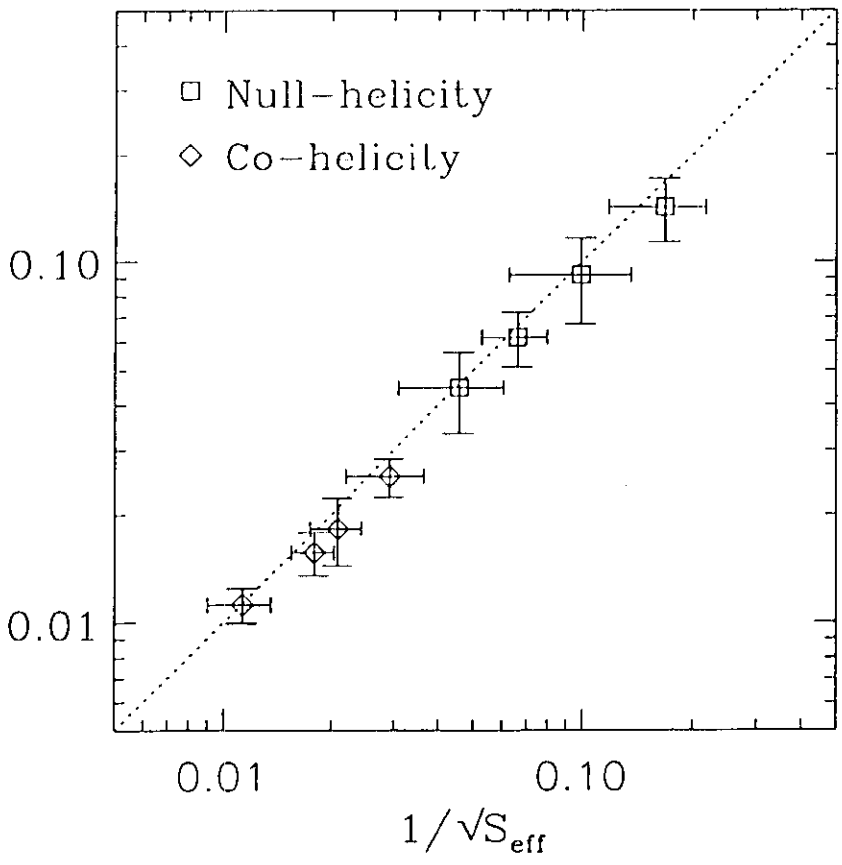

Much slower rates in co-helicity reconnection due to

- **almost no resistivity enhancement**
- **higher down stream pressure**
- **less compressible**

Experimental Test of the Sweet-Parker Model of Magnetic Reconnection

Hantao Ji, Masaaki Yamada, Scott Hsu, and Russell Kulsrud

Princeton Plasma Physics Laboratory, Princeton University, P.O. Box 451, Princeton, New Jersey 08543

(Received 29 September 1997)

We report a quantitative experimental test of the Sweet-Parker model of magnetic reconnection in a controlled laboratory plasma. It is found that the observed reconnection rate can be explained by a generalized Sweet-Parker model which incorporates compressibility, downstream pressure, and the effective resistivity. The latter is significantly enhanced over its classical values in the collisionless limit. [S0031-9007(98)05822-0]

PACS numbers: 52.30.Jb, 94.30.Lr, 96.60.Rd

Magnetic reconnection plays a crucial role in determining the topology of magnetic fields in space and laboratory plasmas [1,2]. Although this is a localized process, it often causes fundamental changes in macroscopic configurations, such as in solar flares [3], magnetospheric substorms [3], and relaxation processes in laboratory plasmas [4]. Magnetic reconnection also provides the most plausible mechanism for releasing the energy stored in the magnetic field to plasma kinetic and thermal energies as observed in solar flares, auroral phenomena, and laboratory plasmas. The concept of magnetic reconnection was first suggested by Giovanelli [5] more than fifty years ago, and the first quantitative model was proposed by Sweet [6] and Parker [7] ten years later. Since then, however, the validity of the Sweet-Parker model has been questioned because its predicted reconnection rate is too slow to explain explosive solar flares. Instead, the attention has shifted to Petschek's model [8] and other models based on standing shock waves [9], which predicted faster reconnection rates. Availability of computer simulation as a research tool has brought about an explosive amount of literature [10] on magnetic reconnection physics in great detail.

Despite the theoretical and computational progress made in past decades on magnetic reconnection, none of these models have been verified or even tested in the laboratory or in space. Stenzel and Gekelman [11] carried out a series of experiments in a linear device and in the electron magnetohydrodynamic (EMHD) regime where *only* electrons are magnetized, while most space plasmas of interest are in the MHD regime where ions are also magnetized. Although detailed local fluctuations were measured in their experiments, quantitative tests of leading theoretical models were not made. More recent experiments have focused on the effects of the third field component during reconnection from both global [12] and local [13] points of view. In this Letter, we report a quantitative experimental test of the Sweet-Parker model in the Magnetic Reconnection Experiment (MRX) [14], where 2D magnetic reconnection is realized in the MHD regime. A significant finding is that the observed reconnection rate can be explained by a generalized Sweet-Parker model which includes compressibility, downstream pressure, and the effective resistivity.

An example of driven magnetic reconnection in MRX is displayed in Fig. 1, where both the measured magnetic field vector $\boldsymbol{B}$ and contours of the poloidal flux Ψ (from radial integration [14] of B_Z) in a single discharge are plotted in an R-Z plane. All results reported here are for the case of antiparallel reconnection in which the toroidal field is negligible. Magnetic reconnection is induced by changing currents in two flux cores whose toroidally symmetric shape ensures the 2D geometry [14]. As the oppositely directed magnetic field lines (B_Z) move toward each other in the R direction, a sharp sheet current develops perpendicular to the plane of the page. The sheet current diffuses due to plasma resistivity in this "diffusion region," where a magnetic field line can lose its original identity and reconnect to another field line. The reconnected field lines (B_R) then move away along the Z direction.

The motion of magnetic field lines in an MHD plasma with resistivity η is described by

$$\frac{\partial \boldsymbol{B}}{\partial t} = \nabla \times (\boldsymbol{V} \times \boldsymbol{B}) + \frac{\eta}{\mu_0} \nabla^2 \boldsymbol{B}, \qquad (1)$$

where $\boldsymbol{V}$ is the flow velocity. The first term on the right-hand side represents the effect of plasma convection while the second term describes field line diffusion. Significance of the diffusion term is represented by $1/S$ where the Lundquist number S is defined by $\mu_0 L V_A/\eta$. Here $V_A \equiv B/\sqrt{\mu_0 \rho}$ (ρ = mass density) is the Alfvén speed and L is the typical plasma size. For typical MHD plasmas such as

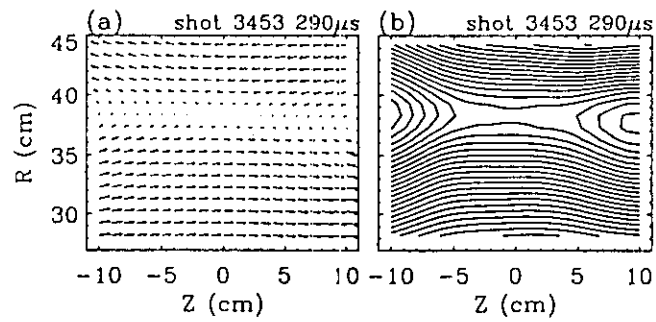

FIG. 1. An example of driven magnetic reconnection measured in a single shot by a 2D probe array: (a) vector plot of poloidal field; (b) poloidal flux contours. Toroidal field (the third component) is negligibly small.

 0031-9007/98/80(15)/3256(4)$15.00

solar flares [3], $S > 10^{10}$; for tokamaks, $S > 10^7$; and for MRX plasmas, $S \lesssim 10^3$.

Another important equation governing reconnection is the continuity equation,

$$\frac{\partial n}{\partial t} + \nabla \cdot (nV) \approx \frac{\partial \bar{n}}{\partial t} - \frac{\bar{n} V_R}{\delta} + \frac{\bar{n} V_Z}{L} = 0, \quad (2)$$

where δ (L) is the thickness (width) of the current sheet and $\bar{n}$ is the averaged density in the diffusion region. V_R (V_Z) is the reconnection speed in the upstream (downstream) region. Integration of the equation of motion in the steady state, $\rho V \cdot \nabla V = -\nabla p + j \times B$ (i.e., the R component along the R direction and the Z component along the Z direction) gives

$$p_{\rm up} + \frac{1}{2}\rho V_R^2 + \frac{B_Z^2}{2\mu_0} - \frac{1}{\mu_0}\int_0^{\delta} B_Z \frac{\partial B_R}{\partial Z}\, dR = p_0 = p_{\rm down} + \frac{1}{2}\rho V_Z^2 + \frac{B_R^2}{2\mu_0} - \frac{1}{\mu_0}\int_0^{L} B_R \frac{\partial B_Z}{\partial R}\, dZ, \quad (3)$$

where p_0, $p_{\rm up}$, and $p_{\rm down}$ are plasma pressures at the center and in the upstream and downstream regions, respectively. The last terms on both sides represent the magnetic tension forces. The original Sweet-Parker model [6,7] assumes steady state reconnection ($\partial B/\partial t = 0, \partial V/\partial t = 0$) in an incompressible plasma ($\nabla \cdot V \propto \partial \bar{n}/\partial t = 0$) with uniform pressure outside the diffusion region ($p_{\rm up} = p_{\rm down}$) and negligible $\rho V_R^2/2$, $B_R^2/2\mu_0$, and tension forces. Then Eqs. (1)–(3) can be reduced to $V_R = \eta/\mu_0\delta$, $V_R = (\delta/L)V_Z$, and $V_Z = V_A$, resulting in a simple expression for the reconnection rate as measured by the Alfvén Mach number, $M_A \equiv V_R/V_A = \sqrt{\eta/\mu_0 L V_A} = 1/\sqrt{S}$.

The Sweet-Parker model can be tested if all the basic plasma parameters are adequately measured. The low temperature (<50 eV) and short-pulsed (<1 ms) MRX plasmas have the advantage that internal probes can be used routinely. Langmuir probes with triple pins measure electron density (n_e) and temperature (T_e) simultaneously. The plasma density measurement has been calibrated by an interferometer which measures the line-integrated density. All three components of B are measured during the reconnection process by a 90 channel 2D pick-up coil array with 4 cm resolution. A finer 1D pick-up probe array with 0.5 cm resolution is used to measure the B_Z profile across the current sheet [13]. The measured B_Z profiles are fit into the Harris-type function [15], $\tanh[(R - R_0)/\delta]$, to determine δ and peak current density. Local flow velocity can be determined either by a Mach probe or time evolution of $\Psi(R, Z)$, i.e., $V_X = -(\partial\Psi/\partial t)/(\partial\Psi/\partial X)$ ($X = R$ in the upstream region and $X = Z$ in the downstream region). The latter method is valid when the resistive effects are negligible, a condition satisfied outside the diffusion region. Results from both methods are in good agreement, and the latter has been used routinely because of its convenience. Probe perturbation of the plasma is estimated quantitatively and observed to be less than 5% [14]. Typical plasma parameters are as follows: $B < 0.5$ kG, $T_e = 10$–20 eV, and $n_e = 0.2$–1.5×10^{20} m^{-3}.

In general, the Lundquist number S is calculated from the measured T_e based on the Spitzer resistivity (parallel resistivity, $\eta_\parallel$). However, perpendicular resistivity $\eta_\perp$ ($= 2\eta_\parallel$) should be used in the case of antiparallel reconnection since the current flows essentially perpendicular to the field. A more detailed calculation which incorporates profile effects of density and temperature gives a nearly identical expression for resistivity [16].

A shot-averaged time evolution of plasma parameters for driven reconnection is shown in Fig. 2. The current density peaks at $t = 290$ μs, when δ is minimized and reconnection speed V_R reaches its steady state of about 3 km/s. The n_e measured at the center of the current sheet keeps increasing until a later time, while T_e at the same location remains almost constant at 10–15 eV (not shown). A series of experiments has been performed in which B_Z is varied while other conditions are kept constant, including the fill pressure $p_{\rm fill}$ (6 mTorr). It is observed that the reconnection rate decreases as B_Z increases.

A straightforward test of the Sweet-Parker model is shown in Fig. 3(a) where the reconnection rate is plotted against $1/\sqrt{S}$. Clearly, the observation does not agree in linear offset nor slope with the Sweet-Parker prediction (dotted line). Causes of these discrepancies can be found by systematically examining the validity of each assumption made in Eqs. (1), (2), and (3).

The first equation to be evaluated is Ohm's law in the toroidal direction, $E_T + V_R \times B_Z = \eta_\perp j_T$, which has been used to derive Eq. (1). All three terms are measured across the current sheet. As shown in the inset of Fig. 4, E_T ($= -\dot{\Psi}/2\pi R$) balances with $V_R \times B_Z$ outside the diffusion region and $\eta_\perp j_T$ inside the diffusion region. In this

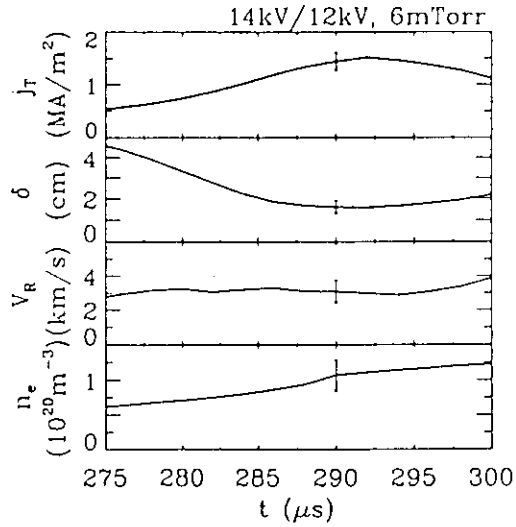

FIG. 2. A shot-averaged time evolution of driven magnetic reconnection. From top: peak current density; current sheet thickness; inflow speed at $R = 30$ cm from flux contour movement; electron density at center.

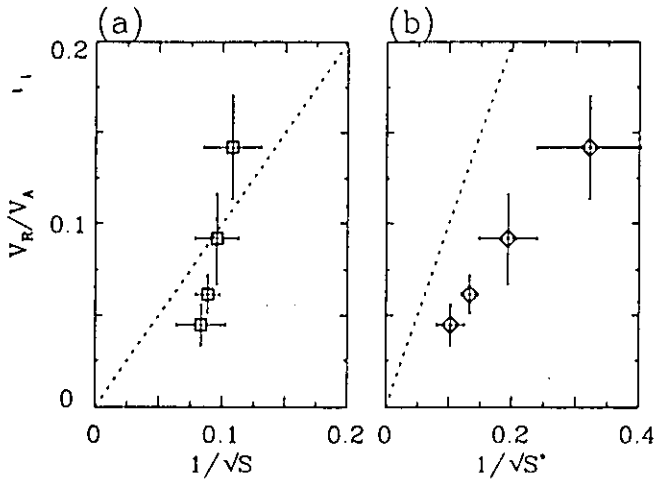

FIG. 3. Experimental test of the Sweet-Parker model (dotted lines): reconnection rate vs (a) $1/\sqrt{S}$ and (b) $1/\sqrt{S^*}$, where S and S^* are calculated from the classical and measured resistivity, respectively.

example, the measured effective resistivity ($\eta_\perp^* = E_T/j_T$) is about twice its classical value. It is found that the enhancement of resistivity is a strong function of collisionality (characterized by the dimensionless parameter λ_{mfp}/δ and dominated by changes in density), as shown in Fig. 4. A significant enhancement ($\sim$10) of the resistivity is observed in the collisionless regime ($\lambda_{mfp} \gg \delta$). We note that electron-neutral collisions are estimated to be negligible compared to Coulomb collisions in the present experimental regimes.

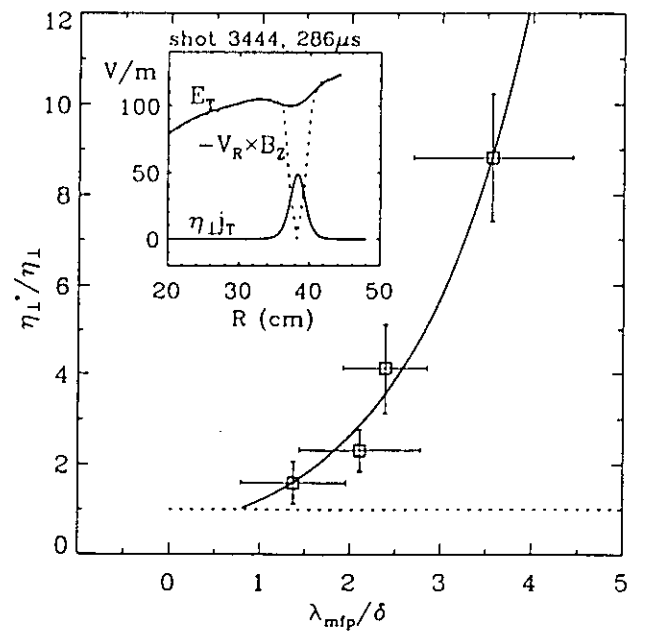

FIG. 4. Resistivity enhancement as a function of collisionality characterized by the ratio of electron mean free path (calculated from n_e and T_e) to current sheet thickness. An example of all three terms of Ohm's law across the current sheet is shown in the inset where $E_T = -\dot{\Psi}/2\pi R$ and V_R is from flux contour movement.

By using $\eta_\perp^*$ to calculate the Lundquist number (denoted by $S^* \equiv \mu_0 L V_A/\eta_\perp^*$), the Sweet-Parker model can be tested again, as plotted in Fig. 3(b). A clear linear dependence can be seen between M_A and $1/\sqrt{S^*}$ (zero offset), but the magnitude is off by a factor of 2. Equation (1) is satisfied since the effective resistivity is used and the steady state assumption ($\partial B/\partial t \approx 0$) holds. Therefore, the discrepancy must reside in the continuity [Eq. (2)] and/or momentum [Eq. (3)] equations.

The incompressibility assumption does not hold since the $\nabla \cdot V$ (or $\partial \bar{n}/\partial t$) term is not negligible compared to the other terms [17] in the continuity equation as seen in Fig. 2, which shows increasing density in the current sheet during reconnection. Retaining this term in the continuity equation leads to an increased inflow, $V_R = (\delta/L)(V_Z + L\dot{n}/n)$, due to an accumulation of density at the center.

Examination of each term in the momentum equation [Eq. (3)] reveals that all assumptions made in the Sweet-Parker model hold approximately true, except that $p_{down} \gg p_{up}$ (dominated by differences in density), as measured by spatial scans of a Langmuir probe. Thus the momentum equation is modified to $V_Z^2 = V_A^2(1 + \kappa) - 2(p_{down} - p_{up})/\rho$, where the outflow is substantially reduced by the higher $p_{down} \sim p_0$. The relative importance of the downstream tension force is represented by $\kappa \equiv (2/B_Z^2)\int_0^L B_R(\partial B_Z/\partial R)\,dZ$ which has been measured to be 0.2–0.3, leading to a slight ($\sim$0.1) increase in the outflow.

As a result, the reconnection rate M_A is modified to $(1/\sqrt{S^*})\sqrt{(1 + L\dot{n}/nV_Z)(V_Z/V_A)} \equiv 1/\sqrt{S_{eff}}$, where the effective Lundquist number is defined as $S_{eff} = (\mu_0 L V_A/\eta^*)/[(1 + L\dot{n}/nV_Z)(V_Z/V_A)]$. The effects of compressibility and downstream pressure can be measured by $L\dot{n}/nV_Z$ and V_Z/V_A, respectively. As S increases, V_Z/V_A decreases to 0.1 $\sim$ 0.2 due to the downstream pressure, while $L\dot{n}/nV_Z$ increases to $\sim$0.4, indicating an increasingly important compressibility effect in a narrower current sheet. Compressibility, which allows local density buildup, explains why higher central density is observed in discharges with higher field even though the initial density is the same.

The observed reconnection rate is plotted against $1/\sqrt{S_{eff}}$ in Fig. 5. As expected, they are in good agreement. The classical Sweet-Parker model needs to be generalized to incorporate the compressibility, the downstream pressure, and the effective resistivity. Effects of the compressibility must be transient (as in MRX) since the density accumulation cannot be sustained indefinitely. However, occurrences of magnetic reconnection in nature do not have to be steady state. They can be impulsive locally while global structures are maintained in a quasi (slowly evolving) steady state, as supported by a recent computer simulation using compressible MHD equations [18].

The effect of downstream pressure is easy to understand. As observed in MRX, higher plasma pressure in the downstream region slows the outflow, thus reducing the reconnection rate. One can envision another case in

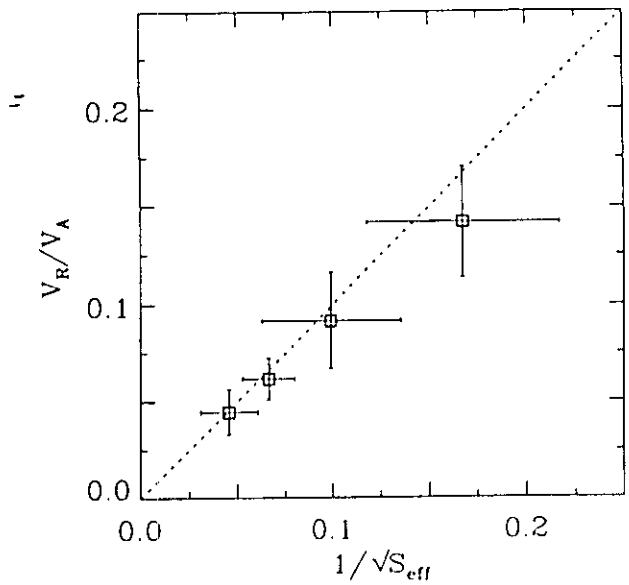

FIG. 5. The observed reconnection rates are compared to the prediction by a generalized Sweet-Parker model, $1/\sqrt{S_{\rm eff}}$, which incorporates finite compressibility, downstream pressure, and the effective resistivity.

which *lower* pressure in the downstream region can result in super-Alfvénic outflow, leading to an *increase* in the reconnection rate, a situation which can exist in solar flares and other cosmic environments.

One relevant question might be whether Petschek-type models can explain the same observations. Direct comparisons, however, are not possible since these shock-based models do not predict definite reconnection rates, only their maxima [1]. Shock structures, a characteristic feature of Petschek-type models, would appear as multiple jumps in $B_Z(R)$ profiles in the downstream region. However, these jumps have not been observed yet within the sensitivity limits of the measurements. We note that the present work neither verifies nor disproves the Petschek-type model. Further tests of these models include searching for shock structures in larger S regimes and investigating the effects of a finite third component [13] and viscosity [19].

In summary we have performed for the first time, to the best of our knowledge, an experimental test of the Sweet-Parker model of magnetic reconnection in a laboratory plasma. It is found that the observed reconnection rate can be explained by a generalized Sweet-Parker model which incorporates compressibility, downstream pressure, and the effective resistivity. A significant implication of this result is that the Sweet-Parker model with generalizations is valid in certain 2D cases. The question of how the resistivity is enhanced in the collisionless limit can be answered only by including fluctuations [20] since all non-fluctuating terms (except E_T and $\eta_\perp j_T$) in the generalized Ohm's law including the Hall and electron pressure terms are estimated to be negligible. Indeed, it is not surprising if current-carrying electrons are scattered by microinstabilities destabilized in the diffusion region, where high current density (therefore large drift parameter) and large inhomogeneity (in plasma pressure and magnetic field) exist. In fact, the drift parameter $v_d/v_{\rm the}$ ($v_d/v_{\rm thi}$), where $v_d = j_T/en$ and $v_{\rm the}$ ($v_{\rm thi}$) = electron (ion) thermal velocity, is found to be a constant ~0.1 (3 to 4) in MRX, independent of the reconnection rate. This suggests that instabilities driven by relative drift between ions and electrons provide a mechanism to limit current density, thus controlling the reconnection rate. However, a complete self-consistent picture for the resistivity enhancement requires fine scale, fully 3D dynamic measurements, which will be a subject of further pursuit in MRX [21].

The authors are grateful to K. Morrison, D. Cylinder, and T. Carter for their technical contributions. This work was jointly supported by NASA, NSF, ONR, and DOE.

[1] V. M. Vasyliunas, Rev. Geophys. Space Phys. **13**, 303 (1975).
[2] D. Biskamp, Phys. Rep. **237**, 179 (1993).
[3] See, e.g., E. N. Parker, in *Cosmical Magnetic Fields* (Clarendon Press, Oxford, 1979); *Introduction to Space Physics*, edited by M. G. Kivelson and C. T. Russell (Cambridge University Press, Cambridge, 1995), and references therein.
[4] See, e.g., J. B. Taylor, Rev. Mod. Phys. **58**, 741 (1986).
[5] R. G. Giovanelli, Nature (London) **158**, 81 (1946).
[6] P. A. Sweet, in *Electromagnetic Phenomena in Cosmical Physics*, edited by B. Lehnert (Cambridge University Press, New York, 1958), pp. 123.
[7] E. N. Parker, J. Geophys. Res. **62**, 509 (1957).
[8] H. E. Petschek, NASA Spec. Pub. **50**, 425 (1964).
[9] B. U. Ö. Sonnerup, J. Plasma Phys. **4**, 161 (1970); E. R. Priest and T. G. Forbes, J. Geophys. Res. **91**, 5579 (1986).
[10] See, e.g., J. F. Drake *et al.*, Phys. Rev. Lett. **73**, 1251 (1994), and references therein.
[11] R. L. Stenzel and W. Gekelman, J. Geophys. Res. **86**, 649 (1981).
[12] M. Yamada *et al.*, Phys. Rev. Lett. **65**, 721 (1990); Y. Ono *et al.*, Phys. Rev. Lett. **76**, 3328 (1996).
[13] M. Yamada *et al.*, Phys. Rev. Lett. **78**, 3117 (1997).
[14] M. Yamada *et al.*, Phys. Plasmas **4**, 1936 (1997).
[15] E. G. Harris, Nuovo Cimento **23**, 115 (1962).
[16] R. M. Kulsrud (to be published); see also S. I. Braginskii, in *Review of Plasma Physics* (Consultants Bureau, New York, 1966), Vol. 1.
[17] The particle source term in the diffusion region is negligible in the present experimental regimes ($p_{\rm fill} \approx 6$ mTorr), but not in discharges with high $p_{\rm fill}$ ($\gtrsim 10$ mTorr).
[18] H. Kitabata *et al.*, J. Phys. Soc. Jpn. **65**, 3208 (1996).
[19] W. Park *et al.*, Phys. Fluids **27**, 137 (1984); H. Ji *et al.* (to be published).
[20] See, e.g., W. H. Matthaeus and S. L. Lamkin, Phys. Fluids **29**, 2513 (1986).
[21] W. M. Tang, Science **279**, 1488 (1998).